Electroplated Metal Microstructures Embedded in Fusion-Bonded Silicon: Conductors and Magnetic Materials

David P. Arnold, *Student Member, IEEE*, Florent Cros, Iulica Zana, *Member, IEEE*, David R. Veazie, and Mark G. Allen, *Senior Member, IEEE*

***Abstract*—Fabrication methods for integrating thick (tens or hundreds of micrometers) electroplated metallic microstructures inside fusion-bonded silicon wafers are proposed and validated. Cu and $Ni_{80}Fe_{20}$ (permalloy) test structures were embedded inside of cavities in silicon wafers, which were fusion-bonded at 500 °C for 4 h with nearly 100% yield. Resistance tests validated the electrical integrity of the metals after annealing, and magnetic measurements indicated the Ni–Fe maintained its magnetic performance after annealing. Additional mechanical tests verified a strong, uniform bond, and that the presence of the metals does not degrade the bond strength. These results demonstrate the ability to integrate conductive and magnetic materials in wafer-bonded silicon, a method useful for a variety of multiwafer, MEMS devices. [1276]**

***Index Terms*—Copper, encapsulation, micromachining, nickel alloys, permalloy, wafer bonding.**

I. Introduction

SILICON wafer bonding is a popular fabrication technique used for a variety of MEMS devices. Initially implemented for creating silicon on insulator (SOI) substrates, it is now commonly employed with bulk silicon etching to form complex, three-dimensional (3-D) structures such as microphones [1], inertial sensors [2], and even multiwafer microengines [3]. These devices use wafer bonding as means to achieve large mechanical structures, fluidic channels, sealed cavities, membranes, floating elements, etc. A good review can be found in [4]. Fusion, or direct, bonding is often preferred to other bonding methods (e.g., anodic, eutectic, polymer, glass frit, etc.) because it is simple and low-cost, eliminates thermal mismatch issues, requires no intermediate layers, and results in a strong, uniform bond. However, fusion bonding of silicon requires chemically clean, polished surfaces, and a post-bond anneal to strengthen the bond. Typically, an RCA clean is performed before bonding, and post-bond annealing is performed at temperatures from 300 °C–1100 °C [5].

Magnetic actuators [6], motor/generators [7], and power converters [8] form a distinctly different class of MEMS devices, in terms of materials, fabrication approach, and integration strategy. Typically magnetic devices are built on a variety of substrates in a surface micromachining fashion, using multilevel metallization of electroplated materials in polymer micromolds [9]. Electrodeposition has proven to be an effective method for building the thick (tens or hundreds of micrometers) conductive and magnetic components to support the high currents and magnetic fluxes required for optimum electromechanic coupling and/or maximum power density.

It follows that magnetic components could be used in tandem with the bulk-micromachined and wafer-bonded silicon structures. When combined, a wide variety of devices are envisioned using magnetic sensing/actuation schemes with complex silicon mechanical structures. Bulk-micromachining and wafer-bonding offer highly 3-D silicon structures with stable and well-characterized mechanical properties. Magnetic sensing/actuation schemes offer high energy density transduction over long coupling distances. Additionally, replacing polymer structures with silicon can enable high temperature devices.

However, the integration of thick metals into a fusion wafer bonding process poses a significant challenge. The high temperatures required for bond annealing demand that oxidation, diffusion, thermal mismatch, and metallurgical/microstructural changes must all be addressed. Additionally, almost all metals are incompatible with the standard RCA prebond cleaning process, so an alternative, metal-compatible preclean needs to be identified. Finally, mechanical tests need to be performed to verify sufficiently strong wafer bonds in the presence of any embedded metal.

The most commonly reported wafer bonding cycle is 1100 °C for one hour under nitrogen in a tube furnace, resulting in a bond strength approaching that of the silicon itself [5]. Many metals used in MEMS devices cannot withstand this temperature (e.g., the melting point of Cu is 1085 °C), but in many cases, such strong bonds are not required. There have been many previous investigations reporting high bond strengths using "low-temperature" silicon-silicon fusion bonding [5], [10]–[16]. The literature offers some processing suggestions for metal-compatibility [14] and shows that a protective oxide layer can be used to protect the silicon surface during various micromachining steps

Manuscript received February 19, 2004. This work was supported in part by the U.S. Army Research Laboratory under the Collaborative Technology Alliance Program (DAAD19-01-2-0010) and the Army Research Office (DAAG55-98-1-0292). The work of D. P. Arnold was also supported by a NSF Graduate Research Fellowship. Subject Editor E. Obermeier.

D. P. Arnold, F. Cros, I. Zana, and M. G. Allen are with the School of Electrical and Computer Engineering, Georgia Institute of Technology, Atlanta, GA 30332-0269 USA (e-mail: gtg776e@mail.gatech.edu; fc29@mail.gatech.edu; iz7@mail.gatech.edu; mark.allen@ece.gatech.edu).

D. Veazie is with the Department of Engineering, Clark Atlanta University, Atlanta, GA 30314 USA (e-mail: dveazie@cau.edu).

Digital Object Identifier 10.1109/JMEMS.2004.835770

TABLE I
METAL-COMPATIBLE PREBOND CLEANING PROCEDURES

Step	Chemicals	Temp. (°C)	Time (min)
1 Organic Clean	1:1:5 NH_4OH:H_2O_2: H_2O	80	10
2 Oxide Etch	(1:6) BOE	25	4 -14*
3 Surface Activation	0.25:1:5 NH_4OH:H_2O_2: H_2O	80	10

* Oxide etch time depends on thickness of oxide; the etch should be stopped immediately after all oxide had been removed.

before bonding [17], but an investigation of embedded electroplated metals in fusion-bonded silicon has not been previously demonstrated.

In this paper, fabrication methods are developed and verified for incorporating thick (tens or hundreds of micrometers) electroplated metals within fusion-bonded silicon. Electrodeposited Cu and Ni–Fe are the two most popular materials for magnetic MEMS devices, and thus were used to verify the process. Cu and $Ni_{80}Fe_{20}$ (permalloy) test structures were embedded inside silicon wafers, which were subsequently fusion-bonded at 500 °C for 4 h with nearly 100% yield. Resistance tests validated the electrical integrity of the metals after annealing, and magnetic measurements indicated that Ni-Fe maintained its magnetic performance after annealing. Additional mechanical tests verified a strong, uniform bond and that the presence of metal does not degrade the bond strength. These results demonstrate the capability to integrate conductive and magnetic metals in fusion-bonded silicon, which can be used for a variety of 3-D, multiwafer, MEMS devices.

II. FABRICATION DEVELOPMENT

This section discusses the development of reliable fabrication procedures for embedding electroplated metals within fusion bonded silicon. Many initial and parallel experiments were performed to guide the development of the fabrication sequence. Although all of the details from these experiments are not reported here, the key results and lessons learned will be discussed throughout.

A. Prebond Clean

The first objective was to identify a metal-compatible prebond cleaning sequence that provided a highly bondable surface without damaging or significantly etching the electroplated metal structures. The sequence used an organic clean, an oxide etch, and an "activation" step to hydrophilicize the silicon surface as shown in Table I. This process is similar to conventional prebond procedures based on the RCA clean, but the metallic ion clean (HCl-based SC2 bath) is omitted and the concentration of NH_4OH is reduced in the activation step to limit oxidation of the metals. Experiments showed that this sequence resulted in a small ($<1\%$), but measurable increase in the resistance of 35 μm thick electroplated Cu and Ni–Fe test structures, which can be attributed to surface oxidation (oxidizing bath) and cross sectional reduction (etching of the generated oxide by HF).

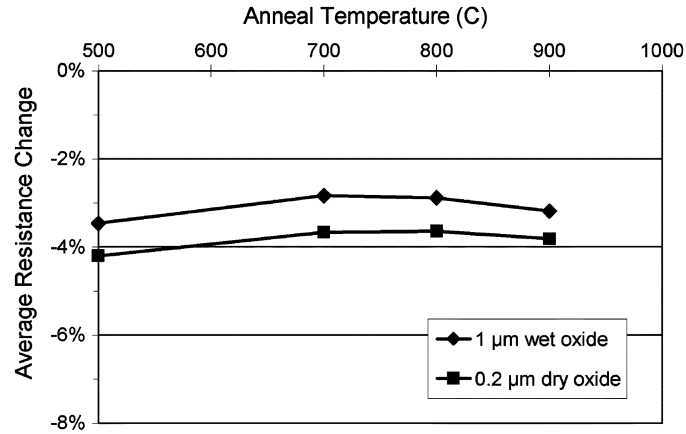

Fig. 1. Resistance change of electroplated Cu test structures on 300 nm Ta diffusion barrier on oxidized silicon wafers after annealing in nitrogen for one hour. The samples showed catastrophic diffusion barrier failure for temperatures above 900 °C.

B. Thermal Limits

Next, experiments were performed to explore the thermal limits of the metals during wafer-bond annealing. If Cu were used as a conductor in a magnetic device, it would typically be dielectrically isolated from the Si substrate by an SiO_2 layer. Diffusion of Cu was considered a crucial factor, as it is known that Cu readily reacts with Si and SiO_2 to form silicide compounds at temperatures as low as 200 °C [18]. Inter-diffusion between the Cu and Si substrate would cause electrical shorts and could not be tolerated. Comprehensive reviews of diffusion barriers between Cu and Si/SiO_2 can be found in [19] and [20]. Ta was selected as a suitable diffusion barrier for its ease of deposition, good adhesion, and reported thin-film diffusion protection up to 650 °C [18]. In the case of Ni–Fe, interdiffusion and interfacial silicide formation were not considered as crucial, as long as the bulk material retained its magnetic properties. These interfacial effects could be tolerated because magnetic isolation would be maintained even if the structure was electrically shorted to the substrate. Therefore, a thin Cr adhesion layer was used instead of Ta, for the Ni–Fe structures.

Measurements were made on electroplated Cu four-point resistive test structures on flat silicon wafers before and after annealing, to emulate the wafer bonding process and determine the survivability of the metal structures. The structures were very similar to the embedded test structures that will be described in detail later. Electroplated Cu lines 30–100 μm wide and 35 μm thick were patterned on a 300-nm dc-sputtered Ta diffusion barrier on top of either a 200-nm dry thermal oxide or a 1-μm wet thermal oxide. Fig. 1 shows the average resistance change after annealing in nitrogen for one hour at temperatures from 500–1000 °C. The structures exhibited good adhesion and a slight decrease in resistance when annealed up to 900 °C, with no appreciable difference between the two oxides. Above 900 °C, the copper failed catastrophically, and energy dispersive X-ray spectroscopy (EDS) analysis revealed the formation of Cu–Si compounds, indicative of diffusion barrier failure. While the nature of the Cu–Ta–Si interfaces and failure mechanism were not fully

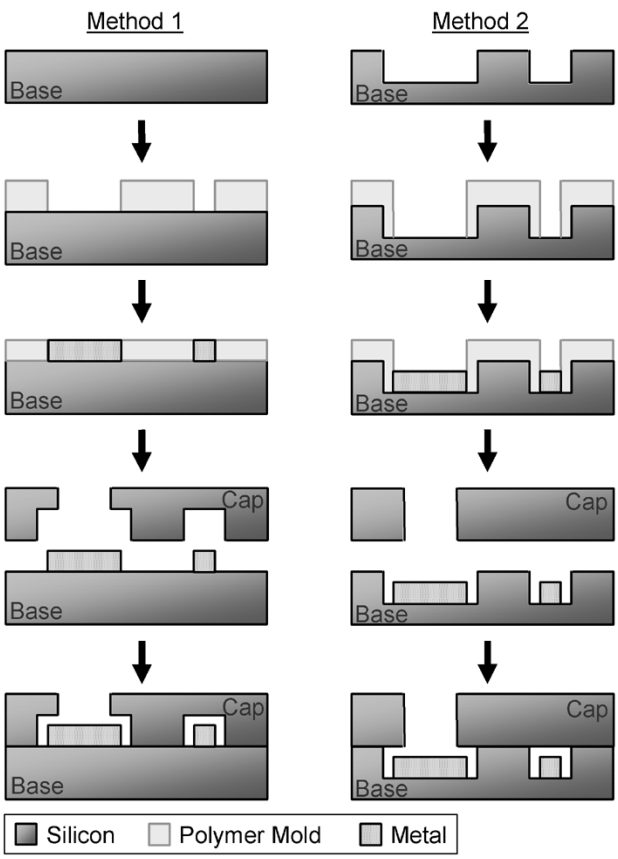

Fig. 2. Alternative fabrication methods for embedding metal in wafer bonded silicon, depicting an embedded line and bond pad with contact opening. Note diffusion, seed, and oxide thin-film layers are not shown.

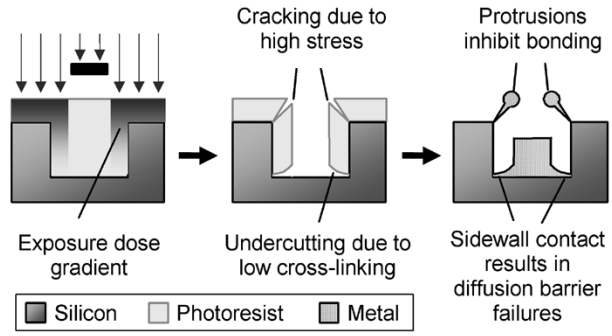

Fig. 3. This schematic depicts two unwanted mold defects when trying to minimize sidewall gap using negative resist. An exposure dose gradient causes high crosslinking of the upper surface and low crosslinking deep in the trench, which can lead to cracking and/or undercutting during development.

explored, these temperatures are higher than the 650 °C limit previously reported for thin films of Cu [18]–[20]. These results demonstrated that Cu could survive the high temperatures for wafer bond annealing.

C. Embedded Metal Process

The next step was to develop a fabrication process for embedding metals within cavities in fusion-bonded silicon. The primary focus was to maintain a pristine silicon bonding surface during all processing before wafer bonding. As a result, fabrication approaches that required polishing of the bonding surfaces were not considered, as the surface roughness and cleanliness are the most important factors for reliable bonds [5]. Two complimentary methods were proposed as shown in Fig. 2. In Method 1, a flat base wafer is electroplated with metal, and another cap wafer with corresponding cavities is bonded around the metal structures. In Method 2, metal is patterned in pre-etched cavities in the base wafer, and a flat cap wafer is bonded to seal the metals inside.

The conceptual fabrication sequence begins by growing a thermal oxide on a flat or pre-etched base silicon wafer. This oxide serves as an electrical insulator for the electroplated metal and as a sacrificial protective layer [17] for the unplated areas, which will later become bonding surfaces. A diffusion/adhesion layer and seed layer are sputtered across the entire wafer. The diffusion barrier prevents interaction of the plated metal with the silicon, and the seed layer ensures a highly conductive surface to initiate the electrodeposition. Thick photoresist is then patterned to define an electroplating mold. In the case of the pre-etched wafers, the pattern is defined down into the trench to prevent electrodeposition on the side walls and overgrowth protrusions that would require polishing. Next, metal is electroplated to the desired thickness and the mold is stripped. The thin films in the nonplated areas are then wet-etched back down to the silicon surface. The cap wafer is prepared separately by etching cavities and/or contact holes in the appropriate locations. Both wafers are then cleaned, aligned, bonded, and annealed. The seed, diffusion layers, etch chemistries, and details of the processing steps for Cu and Ni–Fe will be discussed, but the general procedure is applicable to a variety of electroplated materials.

There are advantages and disadvantages to each method. The challenge for Method 2 is the micromolding and electroplating in cavities in the base wafer. However, this Method 2 does not require an aligned wafer bond (requiring specialized equipment) or a double etch of the cap wafer, as compared to Method 1. Method 2 is also more easily integrated with commonly used wafer bonded structures, and for these reasons, it was selected as the primary method for investigation.

To achieve structures fully recessed in the base wafer using Method 2, a polymer plating mold needed to be patterned within the confines of the cavities. The mold was designed to leave a gap between the metal and the Si sidewall. This helped to reduce thermal stresses and eliminate diffusion barrier failures due to defects in the rough sidewall. The resulting "bottom-up" plating also enhanced uniformity and prevented metal from protruding from the cavity. Futurrex NR9-8000P high aspect ratio negative photoresist was used, but the sidewall gap was limited by cracking and undercutting of the resist as shown in Fig. 3. The subsequent protrusions can inhibit bonding and the sidewall contact in the trench can result in diffusion barrier failures. Cracking and undercutting of the mold were eliminated by maintaining a sidewall gap of at least $1/3$ the trench depth (e.g., 50 μm gap for 150 μm deep cavity) for cavities up to 150 μm deep. It should be noted that SU-8 epoxy was also considered, but the difficulty of removal precluded its use.

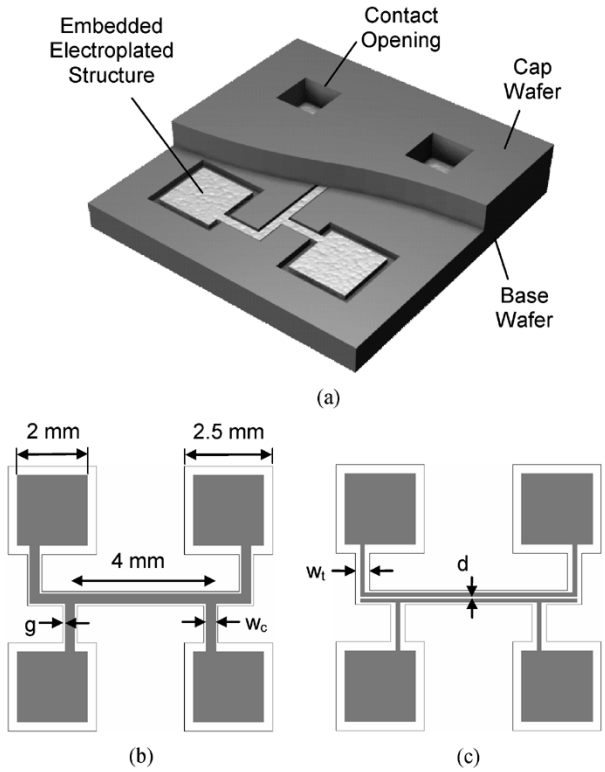

Fig. 4. (a) Rendering of embedded test structure with a cutaway of cap wafer. The accompanying mask patterns for (b) four-point resistive test structure and (c) parallel line test structure are also shown. The variable parameters in the mask set were the conductor width, $w_c = 100$–$320\ \mu m$, trench width, $w_t = 100$–$400\ \mu m$, sidewall gap, $g = 10$–$60\ \mu m$, and parallel line gap, $d = 40$–$60\ \mu m$.

III. Test Structure Fabrication

For verification of this fabrication approach, embedded Cu and Ni–Fe test structures were fabricated using Method 2, described above. It should be noted that during development structures were successfully built using both fabrication methods discussed previously, but only the results using Method 2 are reported here.

Masks were designed with a variety of test structures, which were dimensioned to fit inside of cavities, as shown in Fig. 4(a). These patterns were used to explore the electrical and magnetic properties of the Cu and Ni-Fe after various processing steps. The majority of the structures had four 2×2 mm bond pads and interconnecting lines of various widths ($w_c = 100$–$320\ \mu m$) with various sidewall gaps ($g = 10$–$60\ \mu m$), forming a four-point resistance test structure with an active length of 4 mm [see Fig. 4(b)]. Some contained pairs of lines separated by various distances ($d = 40$–$60\ \mu m$) for testing the isolation between two parallel conductors [see Fig. 4(c)]. Others had only bond pads (no interconnecting lines) and were used for magnetic characterization. Half of the structures had contact openings for access to the bond pads, while the others were completely sealed for mechanical tensile testing.

Both the Cu and Ni–Fe test structures were prepared using standard 100 cm diameter, p-type, $\langle 100 \rangle$ silicon wafers. Fig. 5 shows the fabrication sequence for patterning electroplated metal in cavities on the base wafer and bonding a cap wafer

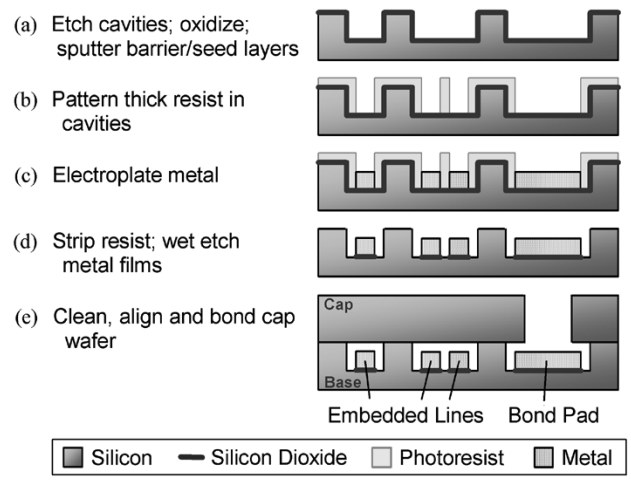

Fig. 5. Fabrication sequence for embedding electroplated metal in base wafer and encapsulating with cap wafer. The cross sections depict examples of single and double embedded lines and a bond pad with a contact opening.

over the cavities. The processes for forming the Cu and Ni–Fe test structures were almost identical, but variations for the Ni–Fe wafer will be denoted in brackets.

The sequence began by growing a $0.2\text{-}\mu m$ dry oxide on the base and cap wafers. This oxide served as a protective layer during all future processing. Clariant AZ4620 photoresist (Somerville, NJ) was then used as a mask for deep reactive ion etching (DRIE) the cavities and contact holes on the base and cap wafers, respectively. The oxide and silicon were etched, forming 75 μm deep cavities in the base wafer and 500 μm deep through-holes in the cap wafer. A post-DRIE piranha clean was performed on both wafers, and the cap wafer set aside.

For the base wafer, a $1\text{-}\mu m$ wet thermal oxide was grown, followed by blanket dc sputtering of a 400-nm Ta diffusion barrier {30 nm Cr adhesion layer}, 200 nm Cu seed layer, and 30 nm Ti adhesion layer [see Fig. 5(a)]. The Ta {Cr} layer limited diffusion and enhanced adhesion, the Cu layer provided a conductive seed layer for electrodeposition, and the upper Ti layer improved adhesion for the subsequent photoresist mold. Next, Futurrex NR9-8000P (Franklin, NJ) negative photoresist was patterned to define the electroplating mold within the confines of the cavities [see Fig. 5(b)]. The limitations of this method were previously discussed. Then, after a brief dip in diluted HF to remove the Ti layer, Cu {Ni-Fe} was electroplated 35 μm thick [see Fig. 5(c)] using standard electrolytic baths [21].

After plating, the resist molds were stripped using Futurrex RR4 (Franklin, NJ). The stripper consistently had a difficult time stripping the samples that had been in the Ni–Fe bath, and additional ultrasonic agitation and oxygen plasma treatment were necessary to remove all of the residues. The thin film Ti, Cu, and Ta {Cr} layers were then selectively wet-etched back down to the SiO_2 layer [see Fig. 5(d)]. Wet etching was preferred over dry etching to prevent particle contamination and micromasking, sometimes encountered when using plasma etching tools. The Ti layer was removed using 1:20 HF:H_2O for ~ 30 s, and the Cu seed was removed using NH_4OH saturated with $CuSO_4$ for ~ 5 min. A wet etch was developed and characterized for the Ta that proved to be quite slow, but sufficiently selective: a 1:1 mixture of H_2O_2:EDTA (1 M) was used at 60 °C

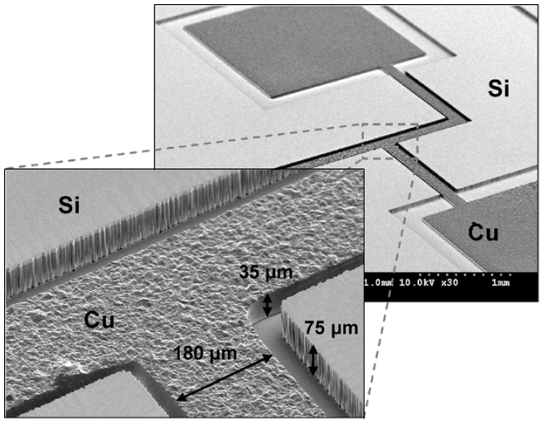

Fig. 6. SEM images of electroplated Cu test structure recessed in a Si cavity before bonding.

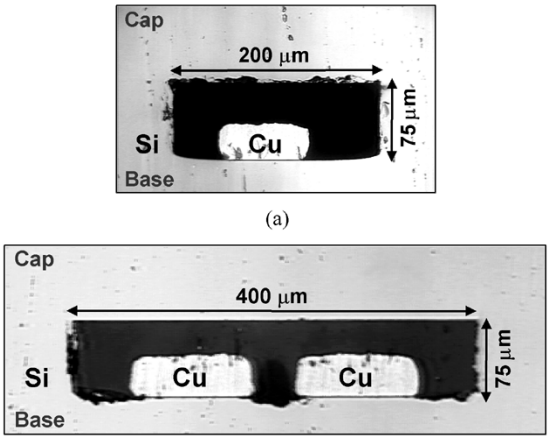

Fig. 7. Optical images showing cross-sections of Cu structures embedded in Si after bonding at 500 °C for 4 h: (a) single buried line and (b) double buried lines. Chipping of the silicon is from dicing/polishing.

for ~3.5 h. [For the Ni-Fe samples, the Cr was removed using a standard chromium etchant (Cyantek, Freemont, CA)]. At this point, only the Cu {Ni–Fe} test structures remained on the SiO_2 layer. Fig. 6 shows an example of the resulting structure recessed in a silicon trench.

Next, both the base and cap wafers were prepared for bonding using the methods outline in Table I. The cap and base wafers were then aligned and contacted at room temperature [see Fig. 5(e)]. The bonded pair was inspected using infrared (IR) transmission imaging and typically indicated >90% bonded area with void regions near the edges of the wafers. Finally, the wafers were annealed using a wafer bonder (Suss Microtec, Germany) at 500 °C for 4 h in vacuum ($<2 \times 10^{-6}$ torr) with 200 kPa clamping pressure. Fig. 7 shows cross-sections of embedded Cu lines after annealing. Postbond IR imaging indicated the bond area had typically increased to nearly 100% as shown in Fig. 8(a). It should be noted that initial attempts for bonding were made in a tube furnace at temperatures up to 900 °C for 1 h under nitrogen or 4% H_2/96% N_2 forming gas, but the resulting bond yield was sometimes unacceptably low (<60% bonded area), as shown in Fig. 8(b). This was possibly due to thermally induced stresses and/or outgassing of the

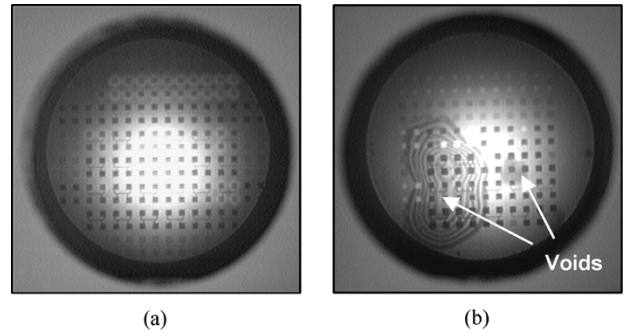

Fig. 8. Typical postanneal IR transmission images of bonded pairs after annealing in (a) wafer bonder (~100% bonded area) and (b) tube furnace (<60% bonded area).

electroplated structures. Switching to the wafer bonding system offered a low-vacuum environment and the use of a physical clamping force. This system improved the bond yield, but limited the temperature to 500 °C. During all low-temperature bonding, no bubble voids were observed, as have been reported in other studies [11]–[13]. The presence of the cavities may act to getter any gases released at the bond interface during bond annealing [11].

IV. Characterization

Using the fabricated embedded structures, electrical, magnetic, and mechanical tests were performed to verify the stability of the metallic materials and strength of the wafer bond.

A. Electrical Tests

The resistances of the test structures were measured before and after bond annealing using a four-point resistance measurement at 1 A as shown in Fig. 9(a). Immediately after contacting, the average resistivities of the Cu and Ni–Fe were $1.79 \pm 0.40\ \mu\Omega \cdot \mathrm{cm}$ and $14.8 \pm 3.6\ \mu\Omega \cdot \mathrm{cm}$, respectively. After bonding at 500 °C for 4 h, an average resistance reduction of 2.6% for the Cu and 23% for the Ni-Fe was measured as shown in Fig. 9(b). The resistance drop corresponds to resistivities of $1.75 \pm 0.39\ \mu\Omega\cdot$ cm and $11.4 \pm 2.8\ \mu\Omega \cdot \mathrm{cm}$ for Cu and Ni–Fe, respectively, and can be attributed to microstructural changes such as grain growth as described in [22]. These results show that the metals survive the wafer bonding process.

Additional measurements were conducted to see if the structures were dielectrically isolated from the substrate. Certain test structures had two parallel lines in the cavity channel. A penetration of the diffusion barrier would result in conduction through the silicon substrate and non infinite-resistance between the two adjacent structures. The Cu structures showed resistance above the limits of the meter used for testing (>20 MΩ) before and after annealing, proving that the Ta diffusion barrier was effective. On the other hand, the Ni-Fe parallel lines showed a short circuit (2–10 Ω) through the substrate, indicative of diffusion. This was not unexpected, as no effort was made to prevent diffusion of the Ni–Fe. It would typically be used as a magnetic structure, and its magnetic properties would be of more importance, as discussed in the next section.

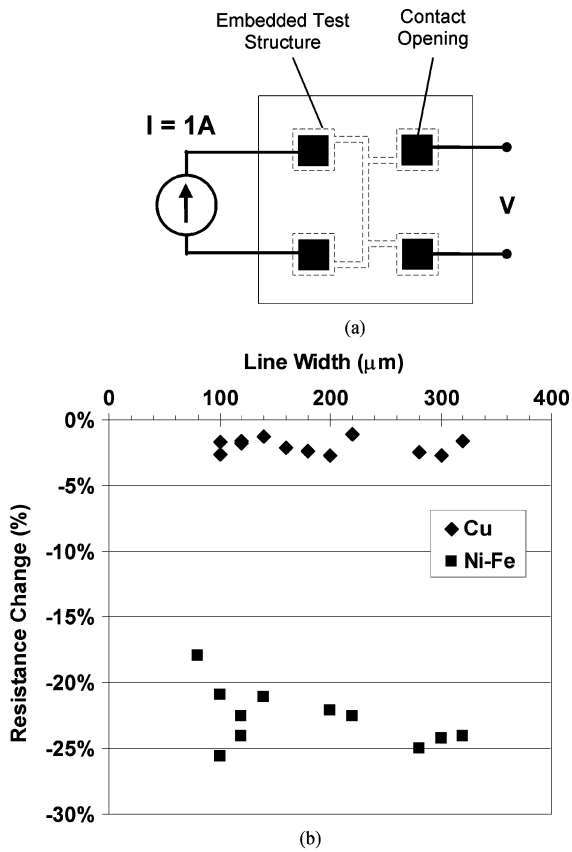

Fig. 9. (a) Four-point resistance measurement of embedded test structure, using a 1-A dc current. (b) DC resistance change of embedded Cu and Ni–Fe of various line widths after bonding (500 °C, 4 h in vacuum).

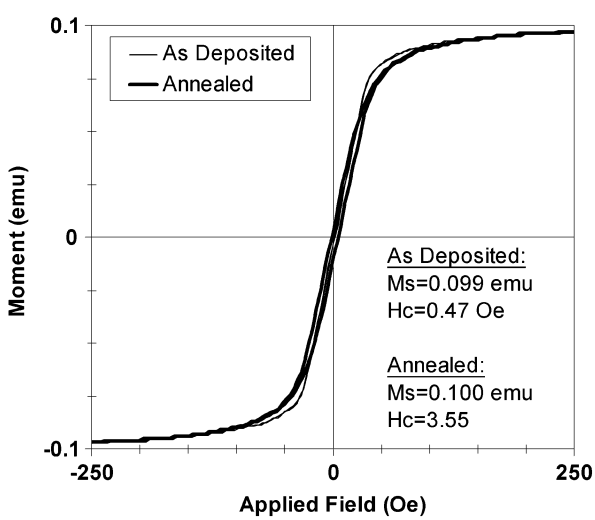

Fig. 10. Magnetization curves for Ni–Fe before and after annealing (500 °C, 4 h in vacuum).

B. Magnetic Tests

To verify that the Ni–Fe material can survive the wafer bond annealing, magnetization measurements were performed using a Lake Shore Model 7300 (Westerville, OH) vibrating sample magnetometer (VSM) on 2 mm × 2 mm square pads of Ni–Fe before and after annealing. The results, shown in Fig. 10, indicate a negligible difference in saturation magnetic moment, but a rise in coercivity from 0.47 Oe (37.4 A/m) to 3.55 Oe (382.6 A/m), which may be attributed to grain growth or stress effects. These results verify that the Ni–Fe maintains its magnetic performance after bond annealing and, therefore, could be employed as an embedded soft magnetic material for various applications.

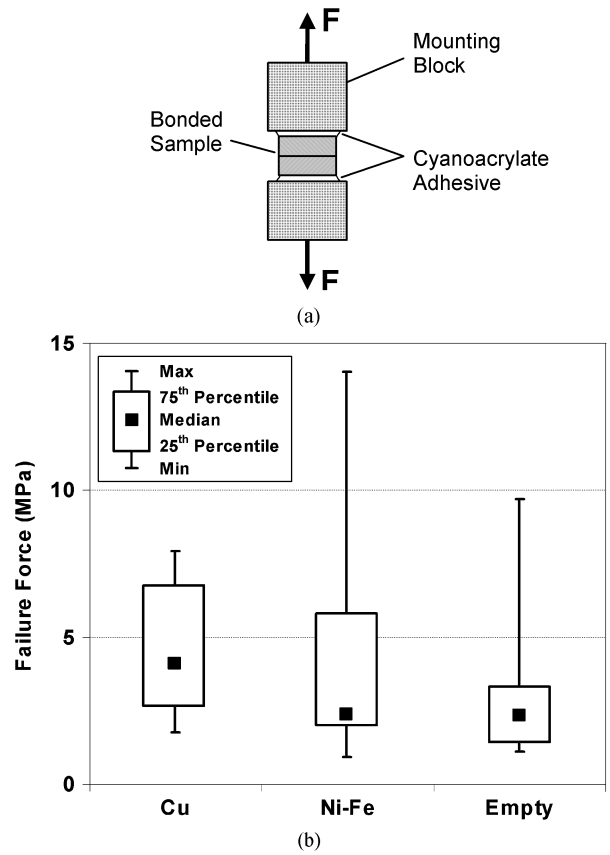

Fig. 11. (a) Method for tensile testing wafer bonded pairs, depicting the bonded sample mounted to the mounting blocks with cyanoacrylate. The debonding force is measured under an applied load. (b) Failure forces for bonded samples with embedded Cu or Ni–Fe compared to bonded samples with empty cavities (500 °C, 4 h in vacuum). Results indicate that the presence of metal does not degrade the bond strength.

C. Mechanical Tests

Last, tensile failure tests [10] were conducted to measure the bond strength and, more importantly, to verify that the presence of the electroplated metal does not adversely affect the quality of the bond. The same test structures with embedded metals were used for these measurements. After bonding at 500 °C for 4 h, the wafers were diced into 1 cm × 1 cm test samples of three different types: cavities with Cu, cavities with Ni–Fe, and empty cavities. The bonded samples were mounted to steel block test fixtures using cyanoacrylate adhesive and tensile loads were applied using an MTS (Eden Prairie, MN) loading frame as shown in Fig. 11(a). The debonding failure force was measured and then divided by the contacted surface area (sample surface area minus cavity area) in order to calculate the bond strength. This mode of bond strength testing has large statistical deviations due to the unstable modes of failure. To best show the variation in the data, the measured bond strengths are shown in quartile format in Fig. 11(b). The mean values (not shown) were 4.6 MPa, 4.6 MPa, and 3.2 MPa for the Cu, Ni–Fe, and

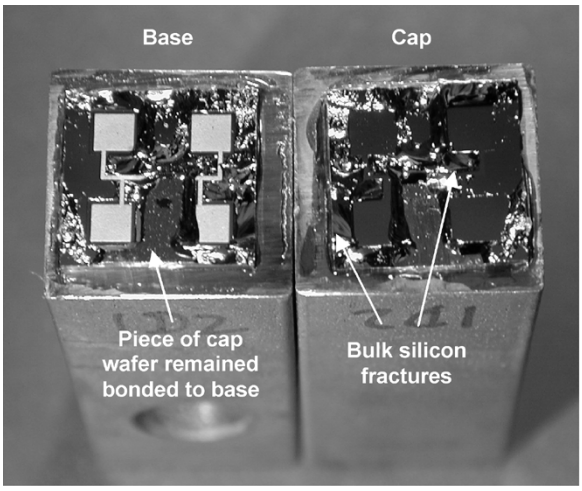

Photograph of base and cap samples on mounting blocks after tensile failure testing. General silicon fractures are evident and a piece of the cap is seen still bonded to the base, indicating a very strong bond.

empty cavities, respectively. Even with the large variations, it is evident that the presence of Cu or Ni–Fe does not reduce the bond strength. Other tests performed early in the development showed average bond strengths of 12.2 MPa could be achieved by bonding at 900 °C for 1 h. However, as stated previously, the yield was quite low due to bond voids and diffusion barrier failures.

Previous investigators report a wide spread of Si-Si bond strengths from tensile failure tests: [10] reported 12–21 MPa after 1 h at 120–400 °C and [14] reported an average of 17 MPa after 4 h at 200 °C, while [12] reported a maximum of 4.25 MPa after several hours at 1000 °C. The bond strengths in this are on the low side when compared to these previous results, but unaccounted for stress concentrations in the nonuniform cross section of the samples may be artificially lowering the "apparent" interfacial force. Nevertheless, the devices could be diced and handled without debonding, and Fig. 12 shows further evidence of a strong, uniform bond. Examination of the bond interface after tensile failure reveals fracture in the bulk silicon, rather than interfacial delamination.

V. Conclusion

This work demonstrates successful fabrication processes for embedding thick electroplated metallic materials in fusion-bonded silicon. The reliability was ascertained through a variety of complementary electrical, magnetic, and mechanical tests. The results show that embedded Cu and Ni–Fe test structures sustain the high temperatures required for bond annealing, and the Si–Si bond strength was unaffected by the presence of the plated materials. These fabrication methods are compatible with a variety of electroplated materials, and are well suited for the construction of magnetic MEMS.

Acknowledgment

The authors thank the staff of the Microelectronics Research Center at the Georgia Institute of Technology for support of the device fabrication. They also thank B. Shonkwiler at Clark Atlanta University for assistance in the mechanical testing.

References

[1] L. Parameswaran, A. Mirza, W. K. Chan, and M. A. Schmidt, "Silicon pressure sensors using a wafer-bonded sealed cavity process," in *Proc. Tech. Dig. 8th Int. Conf. Solid-State Sensors and Actuators (Transducers'95)*, vol. 2, June 1995, pp. 582–585.

[2] B. P. van Drieenhuizen, N. I. Maluf, I. E. Opris, and G. T. Kovacs, "Force-balanced accelerometer with mG resolution, fabricated using silicon fusion bonding and deep reactive ion etching," in *Proc. Tech. Dig. 9th Int. Conf. Solid-State Sensors and Actuators (Transducers'97)*, vol. 2, June 1997, pp. 1229–1232.

[3] A. A. Mehra, A. A. Ayón, I. A. Waitz, and M. A. Schmidt, "Microfabrication of high-temperature silicon devices using wafer bonding and deep reactive ion etching," *J. Microelectromech. Syst.*, vol. 8, pp. 152–160, June 1999.

[4] M. A. Schmidt, "Wafer-to-wafer bonding for microstructure formation," in *Proc. IEEE*, vol. 86, Aug. 1998, pp. 1575–1585.

[5] Q.-Y. Tong and U. Gösele, *Semiconductor Wafer Bonding: Science and Technology*. New York: Wiley, 1999.

[6] C. H. Ahn and M. G. Allen, "A fully integrated surface micromachined magnetic microactuator with a multilevel meander magnetic core," *J. Microelectromech. Syst.*, vol. 2, no. 1, pp. 15–22, Mar. 1993.

[7] H. Koser, F. Cros, M. G. Allen, and J. Lang, "A high torque density MEMS magnetic induction machine," in *Proc. Tech. Dig. 11th Int. Conf. Solid-State Sensors and Actuators (Transducers'01)*, vol. 1, June 2001, pp. 284–287.

[8] J.-W. Park and M. G. Allen, "Ultra low-profile micromachined power inductors with highly laminated Ni/Fe cores: Application to low-megahertz DC-DC converters," *IEEE Trans. Magn.*, vol. 39, pp. 3184–3186, Sept. 2003.

[9] M. G. Allen, "MEMS Technology for the fabrication of RF components," *IEEE Trans. Magn.*, vol. 39, no. 5, pp. 3073–3078, Sept. 2003.

[10] B. Müller and A. Stoffel, "Tensile strength characterization of low-temperature fusion-bonded silicon wafers," *J. Micromech. Microeng.*, vol. 1, pp. 161–166, 1991.

[11] G. Kissinger and W. Kissinger, "Void-free silicon-wafer-bond strengthening in the 200–400 degrees C range," *Sens. Actuators, Phys. A*, vol. A36, no. 2, pp. 149–156, Apr. 1993.

[12] S. N. Farrens, C. E. Hunt, B. E. Roberds, and J. K. Smith, "A kinetics study of the bond strength of direct bonded wafers," *J. Electrochem. Soc.*, vol. 141, no. 11, pp. 3225–3230, Nov. 1994.

[13] Q.-Y. Tong, G. Cha, R. Gafiteanu, and U. Gösele, "Low temperature wafer direct bonding," *J. Microelectromech. Syst.*, vol. 3, no. 1, pp. 29–35, Mar. 1994.

[14] A. Berthold and M. J. Vellekoop, "IC-compatible silicon wafer-to-wafer bonding," *Sens. Actuators, Phys. A*, vol. 60, pp. 208–211, 1997.

[15] Q.-Y. Tong, W. J. Kim, T.-H. Lee, and U. Gösele, "Low vacuum wafer bonding," *Electrochem. Solid-State Lett.*, vol. 1, no. 1, pp. 52–53, 1998.

[16] A. A. Ayón *et al.*, "Characterization of silicon wafer bonding for power MEMS applications," *Sens. Actuators, Phys. A*, vol. 103, pp. 1–8, 2003.

[17] N. Miki *et al.*, "Multi-stack silicon-direct wafer bonding for 3D MEMS manufacturing," *Sens. Actuators: Phys. A*, vol. 103, pp. 194–201, 2003.

[18] T. Laurila, K. Zeng, and J. K. Kivilahti, "Failure mechanism of Ta diffusion barrier between Cu and Si," *J. Appl. Phys.*, vol. 88, no. 6, pp. 3377–3384, Sept. 2000.

[19] S.-Q. Wang, S. Suthar, K. Hoeflich, and B. J. Burrow, "Diffusion barrier properties of TiW between Si and Cu," *J. Appl. Phys.*, vol. 73, no. 5, pp. 2301–2320, Mar. 1993.

[20] T. Laurila, "Tantalum-Based Diffusion Barriers for Copper Metallization," Ph.D. dissertation, Dept. Elect. Comm. Eng., Helsinki Univ. Tech., Espoo, Finland, Dec. 2001.

[21] A. B. Frazier and M. G. Allen, "Metallic microstructures fabricated using photosensitive polyimide electroplating molds," *J. Microelectromech. Syst.*, vol. 2, pp. 87–94, June 1993.

[22] C. H. Seah, S. Mridha, and L. H. Chan, "Annealing of copper electrodeposits," *J. Vac. Sci. Tech. A*, vol. 17, no. 4, pp. 1963–1967, July 1999.

David P. Arnold (S'01) received dual B.S. degrees in electrical and computer engineering in 1999, followed by the M.S. degree in electrical engineering in 2001, from the University of Florida, Gainesville. He is currently pursuing the Ph.D. degree in electrical engineering at the Georgia Institute of Technology (Georgia Tech), Atlanta.

He was awarded fellowships from Tau Beta Pi in 1999 and from the National Science Foundation in 2000. During his fellowship tenure, he developed piezoresistive silicon microphones and MEMS-based acoustic array technologies for aeroacoustic experimentation in the Interdisciplinary Microsystems Group at the University of Florida. In 2002, he began at the Microsensor and Microactuator Laboratory at Georgia Tech, where he is developing magnetic micromachines for microengine power generation. His interests include the design, fabrication, and characterization of magnetic, acoustic, and mechanical microsystems.

Mr. Arnold is also a Member of Eta Kappa Nu and Tau Beta Pi.

Florent Cros received the French B.S. degree in physics and material sciences and the M.S. degree from the National Institute of Applied Sciences, INSA, Toulouse, France, in 1992 and 1997, respectively. He received the Ph.D. degree in microsystems from the Ecole Doctorale de Toulouse, Toulouse, France, in 2002).

He accepted a Postdoctoral position at the Georgia Institute of Technology, Atlanta, focusing on the fabrication of a high-temperature, high- power density micro-induction machine (2002–2003). He has since accepted a position as a Research and Development Engineer at CardioMEMS, Inc., Atlanta, GA.

Iulica Zana (M'98) received the B.S. and M.S. degrees in materials science and engineering from The University "Politehnica" of Bucharest, Romania, in 1994 and 1995, respectively. In 1998, he joined the Center for Materials for Information Technology (MINT), Tuscaloosa, AL, where he worked on deposition and characterization of magnetic thin films. Concurrently, he pursued and received the Ph.D. degree in metallurgical and materials engineering from The University of Alabama, Tuscaloosa, in May 2003.

Since then, he has joined Prof. M. G. Allen's group at Georgia Institute of Technology, Atlanta, as a Postdoctoral Fellow, working on the development and implementation of high performance magnetic materials into new microfabricated magnetic devices. His research interests span from deposition to characterization of magnetic materials.

David R. Veazie received the B.S. degree in mechanical engineering from Southern University in 1986 and the M.S. and Ph.D. degrees in mechanical engineering from the Georgia Institute of Technology, Atlanta, in 1987 and 1993, respectively. His research at Georgia Tech focused on the micromechanical modeling of fiber reinforced composites incorporating distinct interfacial properties.

As a National Research Council (NRC) Postdoctoral Fellow at the NASA Langley Research Center in the Mechanics of Materials Branch, he conducted research on accelerated testing methods and analytical models to predict the long term mechanical properties and durability of high temperature polymer matrix composites. In 1994, he joined Clark Atlanta University's Department of Engineering, Atlanta, GA. He has 10 years experience in mechanical property characterization and durability of composites, accelerated test methods, thermal, and physical aging, environmental effects, fatigue life, and fracture. He manages research projects for DoD, NASA, and industry, including durability modeling for high speed research, impact damage, durability and residual strength of structural composites, microelectromechanical systems, polyimide foams, and multiscale modeling of advanced polymer matrix composites.

Mark G. Allen (M'89–SM'95) received the B.A. degree in chemistry, the B.S.E. degree in chemical engineering, and the B.S.E. degree in electrical engineering from the University of Pennsylvania, Philadelphia, in 1984, and the S.M. and Ph.D. degrees in microelectronic materials from the Massachusetts Institute of Technology, Cambridge, in 1986 and 1989, respectively.

He joined the faculty of the Georgia Institute of Technology, Atlanta, in 1989, where he currently holds the rank of Professor and the J. M. Pettit Professorship in Microelectronics. His research interests are in the areas of micromachining and microelectromechanical systems (MEMS), in particular the development and application of new fabrication technologies for micromachined devices and systems. He was General Co-Chair of the 1996 IEEE MEMS conference, and is North American editor of the *Journal of Micromechanics and Microengineering*.